



## Design, synthesis and biological activity of original pyrazolo-pyrido-diazepine, -pyrazine and -oxazine dione derivatives as novel dual Nox4/Nox1 inhibitors

Francesca Gaggini, Benoît Laleu, Mike Orchard, Laetitia Fioraso-Cartier, Laurène Cagnon, Sophie Hounninou-Molango, Angelo Gradia, Guillaume Duboux, Cédric Merlot, Freddy Heitz, Cédric Szyndralewicz, Patrick Page\*

Genkyotex S.A., 16 Chemin des Aulx, CH-1228 Plan-Les-Ouates, Switzerland

### ARTICLE INFO

#### Article history:

Received 24 May 2011

Revised 4 October 2011

Accepted 7 October 2011

Available online 17 October 2011

#### Keywords:

Pirfenidone

IPF

NADPH oxidase

Nox4

Nox1

Inhibitor

Pyrazolo-pyrido-dione

Antifibrotic

### ABSTRACT

Pyrazolo-pyrido-diazepine, -pyrazine and -oxazine dione derivatives are new chemical entities with good and attractive druglikeness properties. A series of pyrazolo-pyrido-diazepine dione analogs demonstrated to be particularly amenable to lead optimization through a couple of cycles in order to improve specificity for isoforms Nox4 and Nox1 and had excellent pharmacokinetic parameters by oral route. Several molecules such as compound **7c** proved to be highly potent in *in vitro* assays on human lung fibroblasts differentiation as well as in curative murine models of bleomycin-induced pulmonary fibrosis with superior efficiency over Pirfenidone. Pyrazolo-pyrido-diazepine dione derivatives targeting Nox4 and Nox1 isoforms appear highly promising therapeutics for the treatment of idiopathic pulmonary fibrosis.

© 2011 Elsevier Ltd. All rights reserved.

### 1. Introduction

Idiopathic pulmonary fibrosis (IPF) is a chronic progressive parenchymal lung disease that is characterized by the formation of scar tissue within the lungs in the absence of any known cause, and which has a median survival of around 3 years once the condition has been diagnosed but the clinical course can be highly variable.<sup>1,2</sup> Pirfenidone is currently the only therapy specifically approved in Japan and recently in Europe for the treatment of idiopathic pulmonary fibrosis. For many years, the symptoms of the disease were often treated with anti-inflammatory drugs, despite the treatment not producing significant benefit against progression of the disease. One mechanism underlying both the anti-inflammatory and the antifibrotic effects of Pirfenidone may be its ability to suppress the induction and release of inflammatory cytokines. Oxidative stress also enhances the release of cytokines from inflammatory cells. Pirfenidone inhibits NADPH-induced lipid peroxidation

in isolated sheep liver microsomes in a dose-dependent manner. While Pirfenidone is ineffective as a scavenger of superoxide radicals, it is a potent scavenger of hydroxyl radicals. The human therapeutic dose of Pirfenidone used in clinical trials for the treatment of IPF is very high, ranging from 1400 to 2800 mg per day. These high doses are more in favor with a scavenging-based action of Pirfenidone than a targeted drug mechanism of action. Thus, the anti-fibrotic effects of Pirfenidone may be due at least in part to a reduction of oxidative stress induced by toxic hydroxyl radicals.<sup>3</sup>

Increased oxidative stress or increased reactive oxygen species (ROS) production has been implicated in a wide variety of pathologies, including idiopathic pulmonary fibrosis (IPF), kidney fibrosis, diabetic nephropathy, atherosclerosis and neurodegenerative diseases. The relationship between disease progression and overexpression or activation of specific sub-units of Noxes has been shown in many pathologies encouraging the recent development of Nox specific inhibitors.<sup>4</sup>

Amongst the Nox family, the NADPH oxidase isoform 4 (Nox4) has gained considerable and growing attention during the past years. Increasing scientific evidence points to Nox4 as the key source of reactive oxygen species (ROS) in the pathogenesis of idiopathic pulmonary fibrosis. It has been shown that Nox4 is upregulated in both mouse models of IPF and in lung fibroblasts of human IPF patients. Moreover, genetic or pharmacologic silencing

Abbreviations: ADMET, absorption, distribution, metabolism, excretion and toxicity; FITC, fluorescein isothiocyanate; hERG, human ether-a-go-go-related gene; IPF, idiopathic pulmonary fibrosis; NADPH, nicotinamide adenine dinucleotide phosphate; ROS, reactive oxygen species.

\* Corresponding author.

E-mail address: [patrick.page@genkyotex.com](mailto:patrick.page@genkyotex.com) (P. Page).

of Nox4 abrogates fibrogenesis in two murine (bleomycin-induced or FITC-induced) models of lung injury.<sup>5</sup> These studies indicate a crucial role of Nox4 in tissue fibrogenesis and provide proof of concept for therapeutic targeting of Nox4 in fibrotic disorders.

Recently, we have published a large part of our investigation regarding a new class of molecules so-called pyrazolo-pyridine diones targeting the NADPH oxidase isoforms 4 (Nox4) and 1 (Nox1).<sup>6</sup> In this Letter, we would like to complete our work by highlighting sub-chemical series and more specifically new chemical entities so-called pyrazolo-pyrido-diazepine dione derivatives which appear highly promising therapeutics for the treatment of idiopathic pulmonary fibrosis.

## 2. Results and discussion

### 2.1. Chemistry

Our further exploration of the pyrazolo-pyridine dione class<sup>7</sup> is described in the **Scheme 1**: in general, the starting material **1** as chloroacetyl derivatives was easily obtained following the procedure already published on the family of pyrazolo-pyridine dione derivatives.<sup>6</sup> Pyrazolone **1** was subsequently reacted in acetonitrile at 0 °C with different primary diamines **2**: a variety of final compounds were generated according to carbon length ( $n = 1$  and  $2$ ) or substituents ( $R = H$  and  $Ar$ ). Following the pathway A, the intermediate **3** was never isolated ( $R = H, CH_2Ar$  and  $n = 1, 2$ ) as it spontaneously gave the cyclized enamine **4** in situ. When 1,3-propane diamines were used ( $n = 2$ ), a variety of pyrazolo-pyrido-diazepine were obtained. In particular, if  $R = H$ , the enamine intermediate **4** was trapped with Boc anhydride, yielding the resulting compound **5** that was easier purified than its NH precursor. The following cyclization carried out in basic conditions formed the tricyclic compound **6** and the Boc-deprotection was successfully achieved with 4 M HCl solution, affording **7** as HCl salt.

In general, functionalized diamines **2** ( $R = CH_2Ar$ ) were commercially available or prepared through reductive amination.<sup>8</sup> Starting from commercially available aromatic aldehydes and 1,3-propane diamine, the corresponding secondary amines **2** were obtained in good to moderate yields. Isolation of compound **4** with  $R = Ar$  was successfully achieved and its cyclization afforded tricyclic compounds **6** which gave compounds **7** after HCl treatment.

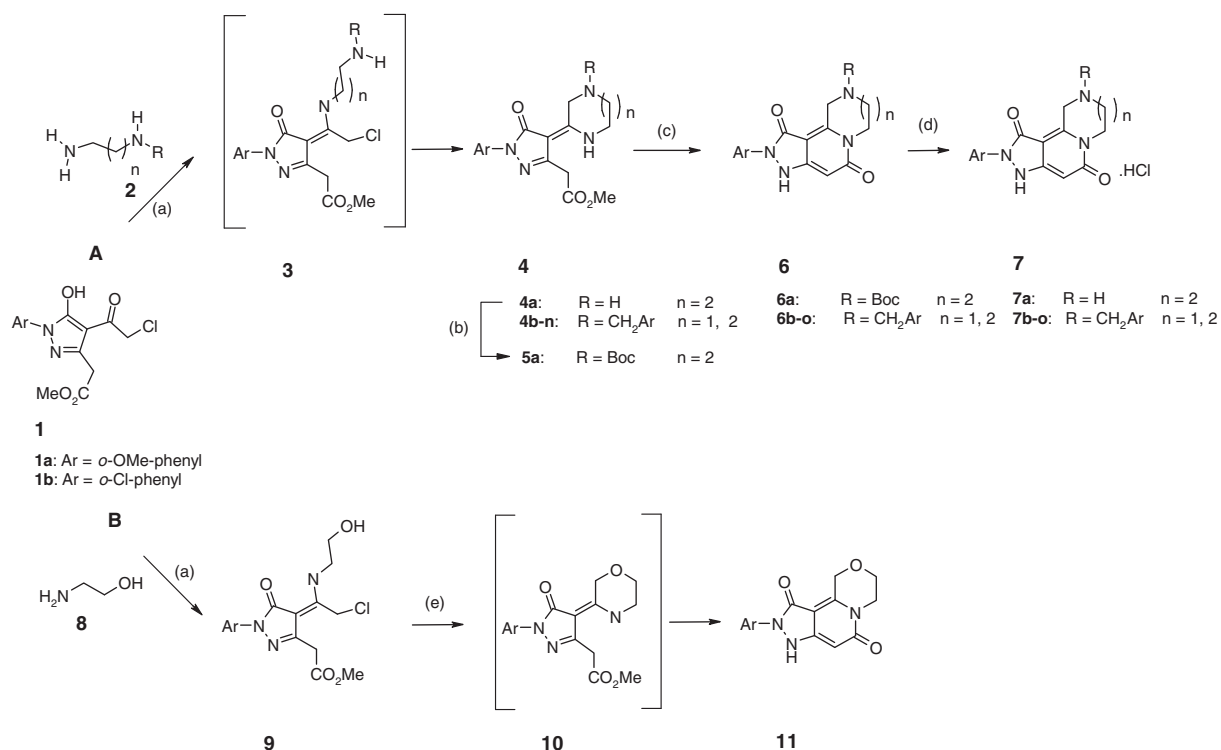
Instead, the synthesis of the piperazine analogs ( $n = 1$  and  $R = H$ ) failed: different reaction conditions and methodologies were used, but unsuccessfully. For example, any attempt of stabilizing the NH-intermediates at all levels (type **4** as NH or **5** as NBoc) gave messy reactions. No improvement was noticed by using the mono Boc-ethylenediamine: chlorine displacement never took place using different reaction conditions such as <sup>t</sup>BuOK/THF or NaH/THF.

We suspected that the difficulties encountered for the synthesis and isolation of these piperazine analogs might be due to their potential instability. Indeed this was confirmed when analog **6** ( $n = 1$ ,  $R = CH_2Ph$ ) was finally made in only 11% yield after tremendous efforts, and found to have poor stability.

A slightly different synthesis was optimized when ethanolamine was used (pathway B, **Scheme 1**). Our starting building block **1** reacted with ethanolamine **8** in acetonitrile at 0 °C, as previously described, allowing the isolation of the intermediate analog **9**. This enamine was directly converted into the final compound **11**: the nucleophilic attack of the alcohol was promoted by NaH/THF and the morpholine-enamine **10** generated the pyrazolo-pyrido-oxazine dione derivatives in situ (pathway B, **Scheme 1**).

### 2.2. Biological results

Based on our previous work identifying the need of specific Nox inhibitors,<sup>6,7</sup> we investigated a new class of molecules whose pyrazolo-pyridine dione core is fused with another ring at the northern part. The six- or seven-member rings closure was ex-



**Scheme 1.** Reagents and conditions: (a) DIPEA, CH<sub>3</sub>CN, 0 °C-RT; (b) Boc<sub>2</sub>O, NaHCO<sub>3</sub>, MeOH; (c) MeOH/MeONa, (d) 4 M HCl, DCM; (e) NaH, THF, 0 °C-RT.

pected to rigidify molecules leading to a diminished number of conformation potentially improving affinity and some ADME parameters such as permeability or metabolism. All compounds were evaluated using our cell free assay of ROS production on human Nox membranes (Nox1, Nox2, Nox4 and Nox5 isoform inhibition data are reported in Table 1).

First of all, the pyrazolone substituent was mostly restricted to the *o*-chlorophenyl group to concentrate the structural investigation on the northern part of the molecule. Initially, neither the size of the cycle attached (six- or seven-membered rings) to the pyridine dione moiety, nor the heteroatom within this ring (*n* or O atom) appeared to have a strong positive impact on the Nox4 or Nox1 specific activities when compared to other pyrazolo-pyridine dione derivatives. Pyrazolo-pyridine dione derivatives with six-membered rings moiety showed interesting functional activity on Nox4 and Nox1 with active compounds **7b** and **11** having  $K_i$  (hNox4) ~142–156 nM. Compound **7b** showed also trends for a better selectivity over Nox2 ( $K_i$  = 2015 nM) and Nox5 ( $K_i$  = 1425 nM). As already described, the inherent chemical difficulties to access easily to pyrazolo-pyridine derivatives with six-membered rings led us to reorganize our strategic chemical efforts.

Consequently we focused on the seven-membered ring derivatives, discovering several molecules with nanomolar inhibition, showing high potency on Nox1 and Nox4. The influence of the substituent on the pyrazolone moiety (left part of the structure) was summarily investigated (replacing the *o*-chlorophenyl by an *o*-methoxyphenyl group) since our previous results demonstrated the importance of an ortho aryl substituent on the pyrazolone moiety to improve metabolic stability.

However, the *o*-methoxyphenyl substitution resulted in a loss of affinity for all Nox enzymes: the  $K_i$  values for Nox1 and Nox4 are higher (i.e.,  $K_i$  (hNox4) = 144 nM for **7d** vs 72 nM for **7c**,  $K_i$  (hNox1) = 218 nM for **7d** vs 101 nM for **7c**) but selectivity towards Nox2 and Nox5 is increased. This trend seemed to be corroborated when comparing compounds **7o** and **7n** with **7i** and **7m**, respectively although the differences in activities remained very modest. The *o*-chlorophenyl group was thus confirmed as the substituent of choice in order to build a series of pyrazolo-pyrido-diazepine dione analogs by varying the northern part of the structure, namely the group attached to the nitrogen atom of the diazepine. Interestingly, removal of the benzyl group attached to the nitrogen atom in compound **7a** appeared to diminish the selectivity towards Nox2 while keeping a comparable Nox4 potency (Nox2/Nox4 selectivity ratio = 4.2 vs 18.6 for **7a** and **7c**, respectively). The introduction of a Boc protecting group in compound **6a** restored the Nox2/Nox4 selectivity ratio to 12.4. Overall, increasing steric hindrance by introducing lipophilic groups on the nitrogen of the seven-membered rings seemed to increment selectivity towards Nox2.

On the other hand, substitution by a chlorine atom in *o*-, *m*-, or *p*-position of the benzyl group attached to the diazepine moiety revealed to be well tolerated with  $K_i$  (hNox4) = 76, 101 and 103 nM for **7e**, **7f** and **7g**, respectively. These compounds had also pretty acceptable selectivity over Nox2 and Nox5.

No significant difference was noted when incorporating an *o*-, *m*-, or *p*-methoxybenzyl group with  $K_i$  (hNox4) in the range of 111–116 nM but higher selectivity towards Nox2 and Nox5 for compounds **7h**, **7i** and **7j** (i.e., **7h** vs **7e**; **7j** vs **7g**; and **7i** vs **7f**). This showed as well that the nature of the substituent on the benzyl group is not paramount. Indeed no dramatic differences in potency result from the introduction of a lipophilic entity or hydrogen bond acceptor.

Having found that various benzylic substituents led to potent Nox4/Nox1 inhibitors, the introduction of heterocyclic moieties was then considered for the northern diazepine part of the molecule. Once again, this kind of substitution was tolerated: for instance,  $K_i$  (hNox4) = 111 nM for **7k** bearing a furyl group.

Encouragingly, the picolyl derivatives were found to be very potent on hNox4, particularly in the case of *ortho*-substitution ( $K_i$  = 67 nM for **7m**). The beneficial effect of this *o*-picolyl group might be seen as well with the slight improvement in potency observed when moving from compound **7d** ( $K_i$  = 144 nM) to **7n** ( $K_i$  = 93 nM).

Among the selected compounds, the most active on Nox2 appeared to be the one deprived of substituent on the northern part of the molecule (e.g., **11** and **7a** with  $K_i$  = 433 and 400 nM, respectively). Besides having an *o*-methoxyphenyl-pyrazolone group on the western part of the molecule seemed to increase the potency on Nox2 (**7d**, **7n** and **7o**). All the compounds fall in the same range regarding Nox1 potency ( $K_i$  ~87–398 nM) with benzylchloro diazepine derivatives being the most active along with **7c** and the one harboring an *o*-methoxyphenyl-pyrazolone group the least potent molecules. Concerning Nox5, having a heteroaromatic ring attached to the diazepine moiety brought a detrimental effect (furan, pyridines) whereas molecules without northern substituent were found to be the most active on this Nox isoform.

Similarly to pyrazolo pyridine dione derivatives described in our previous paper,<sup>6</sup> Nox1 and Nox4 functional potency seemed also to be correlated in the pyrazolo-pyrido-diazepine, -pyrazine and -oxazine dione chemical series, which is most likely due to key common interactions related to the central core. Nox2/Nox4 and Nox5/Nox4 selectivity appeared to be acceptable for most tested compounds. As a result these derivatives present relatively similar Nox profiles and appeared to be dual Nox4/Nox1 inhibitors with selectivity over the isoform Nox2. A counter-screening assay Xanthine/Xanthine oxidase was performed on all the molecules to rule out potential scavenging properties and proved to be negative for all of them.

Further investigations did not allow to determine clear-cut optimal substituent for the northern part of the molecule, the most active compounds were then subjected to in vitro profiling, in particular with respect to oxidative metabolism in human and rat liver microsomes, Caco-2 cellular permeation model as well as plasma protein binding assay (see Table 2). Compound **7a** was not selected because of some inappropriate physicochemical properties such as a very low  $\log D$  = -0.38, predicting the compound to be eliminated with a high renal clearance.

Good correlation between  $\log D$  and metabolic clearance was observed for all tested compounds. Most compounds were fairly resistant to oxidative first-pass metabolism, demonstrating medium clearance for both species studied:  $\leq 35.0$  and  $\leq 64.0$   $\mu\text{L}/\text{min}/\text{mg}$  protein in human and rat liver microsomes, respectively. However, notable exceptions were the three derivatives with a chlorobenzyl group attached to the diazepine part: compounds **7e**, **7f** and **7g**. Their low microsomal stability is presumably due to their higher lipophilicity ( $\log D$  = 2.76) that renders them liable to phase I oxidative metabolism, regardless of their substitution (*o*-, *m*- and *p*-Cl).

Concerning the in vitro permeability in Caco-2 experiments, compounds **7l**, **7m** and **7n** harboring a pyridine group revealed to have weak permeability properties associated with a high efflux ( $P_{\text{app}} \sim 1.0\text{--}1.8 \cdot 10^{-6}$  cm/sec and efflux ratios ~10.1–18.7). This can be explained by the relatively low  $\log D$  (<1.1) associated to these compounds and also by the possible protonation of the basic pyridine nitrogen atom, as second basic center in these molecules, which can preclude them to cross readily the lipophilic membranes. We have not investigated whether these compounds might be substrate of transporters potentially providing explanation of the observed efflux. Increasing the lipophilicity of the diazepine substituent with compound **7i** by 1.5–2.0  $\log P$  unit led to a suitable permeability with a very modest efflux ratio. Interestingly, the physicochemical properties of **7c** allowed us to reach a high permeability range for this molecule ( $P_{\text{app}} 42.2 \cdot 10^{-6}$  cm/sec) with no efflux at all.

**Table 1**  
Nox profile of compounds **6a**, **7a–o** and **11**

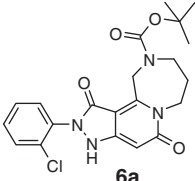
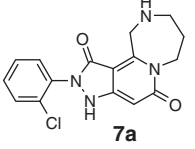
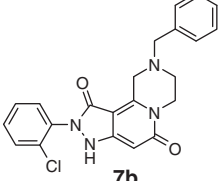
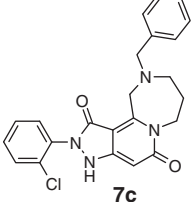
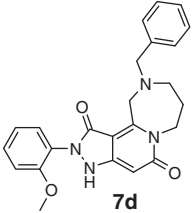
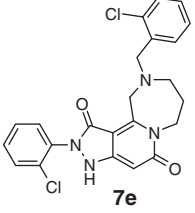
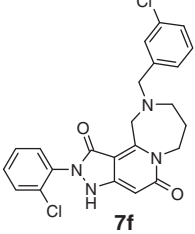
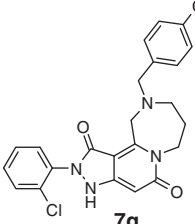
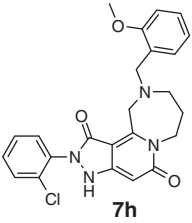
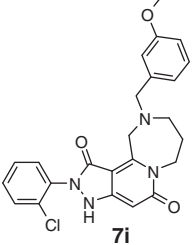
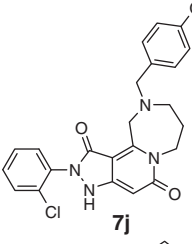
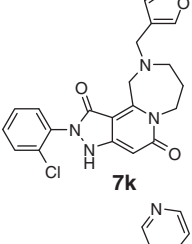
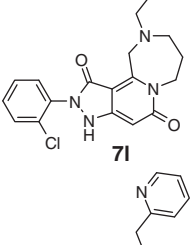
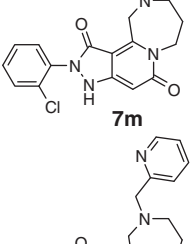
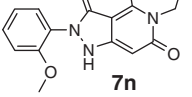
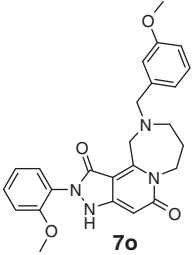
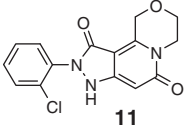
Compound	$K_i$ Nox1 (nM) <sup>a</sup>	$K_i$ Nox2 (nM) <sup>a</sup>	$K_i$ Nox4 (nM) <sup>a</sup>	$K_i$ Nox5 (nM) <sup>a</sup>
 <b>6a</b>	148 ± 18	1280 ± 25	103 ± 12	590 ± 100
 <b>7a</b>	119 ± 20	365 ± 5	87 ± 8	360 ± 74
 <b>7b</b>	398 ± 63	2015 ± 155	142 ± 20	1425 ± 175
 <b>7c</b>	101 ± 10	1340 ± 270	72 ± 3	414 ± 52
 <b>7d</b>	218 ± 39	645 ± 75	144 ± 22	670 ± 30
 <b>7e</b>	87 ± 4	1160 ± 340	76 ± 3	615 ± 175
 <b>7f</b>	104 ± 4	1150 ± 500	101 ± 7	475 ± 65
 <b>7g</b>	95 ± 6	1260 ± 490	103 ± 10	585 ± 225

Table 1 (continued)

Compound	$K_i$ Nox1 (nM) <sup>a</sup>	$K_i$ Nox2 (nM) <sup>a</sup>	$K_i$ Nox4 (nM) <sup>a</sup>	$K_i$ Nox5 (nM) <sup>a</sup>
 <b>7h</b>	133 ± 15	1760 ± 200	111 ± 10	740 ± 90
 <b>7i</b>	113 ± 21	1195 ± 255	112 ± 17	730 ± 100
 <b>7j</b>	184 ± 24	780 ± 170	116 ± 9	690 ± 10
 <b>7k</b>	200 ± 31	1020 ± 190	111 ± 6	955 ± 145
 <b>7l</b>	208 ± 46	1370 ± 80	94 ± 7	1150 ± 170
 <b>7m</b>	113 ± 1	1140 ± 150	67 ± 3	543 ± 26
 <b>7n</b>	217 ± 18	510 ± 20	93 ± 11	610 ± 40

(continued on next page)

Table 1 (continued)

Compound	$K_i$ Nox1 (nM) <sup>a</sup>	$K_i$ Nox2 (nM) <sup>a</sup>	$K_i$ Nox4 (nM) <sup>a</sup>	$K_i$ Nox5 (nM) <sup>a</sup>
 <b>7o</b>	212 ± 51	820 ± 150	131 ± 6	690 ± 60
 <b>11</b>	173 ± 14	433 ± 19	156 ± 11	490 ± 67

<sup>a</sup> Cell free assay of ROS production on membranes over-expressing human Nox.

Table 2

In vitro profiling for selected pyrazolo-pyrido-diazepine dione derivatives

Compound	Cl (h-LM) <sup>a</sup> μL/min/mg protein	Cl (r-LM) <sup>b</sup> μL/min/mg protein	Caco-2 (Papp) <sup>c</sup> (10 <sup>-6</sup> cm/sec)	Efflux ratio	logD <sup>d</sup>	Fu <sup>e</sup>
<b>7c</b>	35.0	64.0	42.2	0.48	2.23	12.0
<b>7e</b>	87.1	164.0	—	—	2.76	—
<b>7f</b>	81.4	153.0	—	—	2.76	—
<b>7g</b>	77.3	152.0	—	—	2.76	—
<b>7i</b>	35.0	60.1	22.3	1.91	1.99	90.1
<b>7l</b>	21.0	31.1	1.0	18.7	0.92	2.9
<b>7m</b>	13.9	27.5	1.8	10.1	1.10	2.6
<b>7n</b>	15.7	32.1	1.4	16.8	0.33	6.9

<sup>a</sup> Microsome stability experiment. h-LM, human liver microsomes.

<sup>b</sup> Microsome stability experiment. r-LM, rat liver microsomes.

<sup>c</sup> Caco-2 cell permeability assay. Papp, permeability coefficient.

<sup>d</sup> Calculated at pH 7.4.

<sup>e</sup> Fraction unbound, plasma protein binding assay in rat (in 50% plasma protein).

The results from these in vitro microsome stability and Caco-2 permeability studies encouraged us to avoid chlorobenzyl or picolyl groups attached to the diazepine moiety but using a simple benzyl or methoxybenzyl group.

Concerning the in vitro plasma protein binding in rat species, similar results were obtained for the very close structural analogs **7l** and **7m**: the free fractions recorded were 2.6% and 2.9%, respectively in 50% plasma protein. Compound **7n** had a higher free fraction (6.9%) presumably due to its lower logD (0.33). On the other hand, the unbound fraction of **7i** revealed to be particularly high (90.1%) despite its average logD (1.99). Associated with a medium metabolic clearance, this data did not encourage us to push this compound forward. Fortunately, its analog **7c** with a logD in the same range (2.23) showed a reasonable free fraction (Fu ~ 12%).

Finally, it is noteworthy to mention that no problem was encountered regarding CYP inhibitions for all-tested compounds having IC<sub>50</sub> >25 μM (data not shown).

On the basis of the data gathered, two compounds were selected for further investigation through their pharmacokinetic properties in rat to help guide selection of a superior clinical candidate. In spite of disappointing in vitro results regarding Caco-2 permeability, compound **7m** was chosen since it was the most potent compound on hNox4 with no other problem spotted during its in vitro profiling. Compound **7c** embodied a good compromise between microsomal metabolism, free fraction, permeability, physical properties associated with high Nox4/Nox1 potency and the highest Nox4/Nox2 selectivity ratio (18.6). The results are combined in Table 3.

Remarkably, the pharmacokinetic profile of **7m** was reasonably good despite the questions raised by its relatively poor in vitro permeability properties and a slightly low logD (1.10). This compound presents indeed acceptable in vivo clearance, plasma concentrations and oral bioavailability ( $F_z = 42\%$ ) and acceptable volume of distribution into tissues ( $V_{ss} = 0.47$  L/kg after iv dosing). Even more interestingly, compound **7c** showed higher exposure presumably due to its good physicochemical properties and higher permeability ranking. Moreover this compound has a suitable oral bioavailability ( $F_z = 53\%$ ) associated with a relatively low in vivo clearance in line with in vitro data. Half-life of 2.71 and 2.37 h were observed after intravenous and per os administrations, respectively, as well as limited but acceptable distribution into tissues ( $V_{ss} = 0.28$  L/kg).

The Nox specificity of **7c** was confirmed in a counter-screening assay for potential ROS scavenging (Table 4) and no potential problem was found regarding CYP450 inhibition. This molecule was not mutagenic nor genotoxic according to mini Ames and in vitro micronucleus tests. It showed as well low probability to generate QT prolongation based on lack of inhibition of hERG. A NOAEL (No Observed Adverse Effect Level) of 1000 mg/kg was determined in mice after 2 weeks daily oral administration. Consequently, this excellent early in vitro ADMET profile confers to this compound a very large safety window.

**7c** abrogates strongly lung fibrosis following a once-a-day oral administration from days 10 to 25 after bleomycin intratracheal administration in a curative model of bleomycin-induced pulmonary fibrosis. Collagen deposition was inhibited by 64% at the dose of 10 mg/kg po with **7c**; the benchmarked Pirfenidone in the same

**Table 3**  
In vivo pharmacokinetic profile in rats for selected compounds

Compound	Route	Dose (mpk)	AUC <sub>∞</sub> (h · ng/mL)	Fz (%)	C <sub>max</sub> (ng/mL)	T <sub>max</sub> (h)	t <sub>1/2</sub> (h)	Cl (L/kg/h)	V <sub>ss</sub> (L/kg)
<b>7c</b>	iv	5	39266	—	42336	—	2.71	0.13	0.28
	po	10	41430	53	14877	0.33	2.37	0.26	—
<b>7m</b>	iv	5	11819	—	21827	—	5.62	0.46	0.47
	po	10	9901	42	11298	0.25	3.63	1.02	—

**Table 4**  
Early in vitro ADMET profile of compound **7c**

IC <sub>50</sub> (1A) <sup>a</sup>	>25 μM
IC <sub>50</sub> (2C19) <sup>a</sup>	>25 μM
IC <sub>50</sub> (2C9) <sup>a</sup>	>25 μM
IC <sub>50</sub> (2D6) <sup>a</sup>	>25 μM
IC <sub>50</sub> (3A4) <sup>a</sup>	>25 μM
K <sub>i</sub> Xanthine oxidase <sup>b</sup>	>30000 nM
hERG <sup>c</sup>	8.7% at 1 μM
Mini AMES test <sup>d</sup>	Negative
In vitro micronucleus <sup>e</sup>	Negative

<sup>a</sup> Inhibition of cytochrome P450 isoforms (see Section 4).<sup>b</sup> In vitro enzymatic assay.<sup>c</sup> Conventional patch-clamp.<sup>d</sup> Performed @ 100 μM.<sup>e</sup> Performed @ 500 μM.

model partially inhibited collagen deposition by 12% only at the dose of 100 mg/kg po (see Fig. 1). A rough estimation of Human Equivalent Dose (HED) by conversion of animal doses, based on body surface area as per the FDA guidance for industry 2002, predicts an orally pharmacologically active dose in human of 50–60 mg once-a-day.

### 3. Conclusion

We have identified a novel family of highly potent dual Nox4/Nox1 inhibitors with selectivity over the isoform Nox2. This investigation was devoted to the pyrazolo-pyrido-diazepine dione derivatives with particular focus on the diazepine moiety. A variety of compounds showed excellent potency in our cell free assay of ROS production on human Nox4/Nox1 membranes. Further improvement of the physical properties and pharmacological pro-

files led to the identification of the highly potent, orally bioavailable **7c**. This compound benefits not only from a straightforward synthetic procedure but also from an excellent pharmacological and safety profile with K<sub>i</sub> in the two digit nanomolar range on Nox4. This compound proved to be highly potent in in vitro assays on human lung fibroblast differentiation as well as in preventive and curative murine models of bleomycin-induced pulmonary fibrosis, where it demonstrates a superior efficiency to Pirfenidone which is today the only drug accepted for the treatment of IPF in Japan and Europe. **7c** deserves clinical trials for the treatment of idiopathic pulmonary fibrosis.

## 4. Experimental section

### 4.1. Chemistry

All solvents used in these reactions were anhydrous and obtained from commercial sources. All other reagents were used as supplied unless otherwise stated. All reactions with moisture sensitive compounds were carried out under nitrogen. Melting points were measured with a Büchi Melting Point B-540 apparatus and were uncorrected. NMR-spectra were recorded on a Bruker AMX-500 and 400 MHz spectrometers. Chemical shifts were expressed in parts per million ( $\delta$ ) and referenced with respect to the residual solvent signal (DMSO: 2.50 ppm). Data were reported as follow: chemical shift ( $\delta$ ), integration, multiplicity (s = singlet, bs = broad singlet, d = doublet, t = triplet, dd = doublet of doublets, ddd = doublet of doublet of doublets, dt = doublet of triplets, td = triplet of doublets, q = quadruplet and m = multiplet) and coupling constants (*J*) in Hertz. UPLC (Ultra Performance Liquid Chromatography) data provided were obtained using a Waters Acquity SQ detector operated in positive or negative electrospray. Analytical HPLC data were obtained using a Waters 2690 separation module (Alliance) equipped with a Zorbax Extend C-18 column (50 × 4.6 mm, 1.8 μm). Detection was conducted at 254 nm and full scan at 210–400 nm with a photodiode array detector. The mobile phase was a linear gradient with a flow rate of 0.8 mL/min using a 10:90 A/B to 100:0 A/B mixture over 4 min. Solvent A was 0.1% formic acid in water, and solvent B was 0.1% formic acid in acetonitrile. Silica flash and reverse phase chromatography were done using the Armen Spot Flash instrument equipped with silica SI60 15–40 μm and RP18 25–40 μm cartridges, respectively. For TLC (thin layer chromatography) alumina sheets from Merck coated with silica gel 60 F254 were used. Reported yields were not optimized, because of our requirement for purity rather than quantity of product.

### 4.2. Synthesis

Synthesis of starting materials **1a**: methyl [4-(chloroacetyl)-5-hydroxy-1-(2-methoxyphenyl)-2,3-dihydro-1H-pyrazol-3-yl]acetate and **1b**: methyl [4-(chloroacetyl)-1-(2-chlorophenyl)-5-hydroxy-1H-pyrazol-3-yl]acetate) were obtained according to the general procedure described in our previous publication.<sup>6</sup>

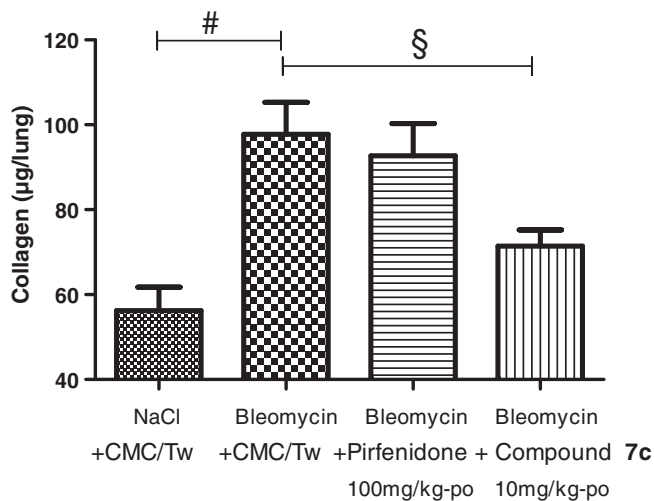


**Figure 1.** Curative model of Bleomycin for compound **7c**. (a) Values are expressed as mean SEM, #*p* < 0.001 compared sham/control bleomycin, §*p* < 0.05 compared compound **7c**/control bleomycin *n* = 8–13 animals.

#### 4.2.1. Synthesis of *tert*-butyl 2-(2-chlorophenyl)-1,5-dioxo-2,3,5,8,9,11-hexahydro-1*H*-pyrazolo[4,3':3,4]pyrido[1,2-*a*][1,4]diazepine-10(7*H*)-carboxylate (**6a**)

Pyrazolone **1b** (0.94 mmol, 322 mg.) was dissolved in acetonitrile (5 mL) and cooled down to 0 °C. Propane 1,3-diamine (0.85 mmol, 63 mg) was slowly added and the reaction was stirred at 0 °C for 1 h. The solvent was concentrated in vacuo and the crude was partitioned between ethylacetate and a saturated solution of NaHCO<sub>3</sub>. The combined organic phases were dried over Na<sub>2</sub>SO<sub>4</sub> and concentrated in vacuo yielding dark oil which was used in the following step without further purification. LC–MS (M+H)<sup>+</sup>: 363.1.

The oil deriving from the previous step was dissolved in methanol, cooled down to 0 °C and NaHCO<sub>3</sub> (71 mg, 0.85 mmol) was added. Boc<sub>2</sub>O (185 mg, 0.85 mmol) was dissolved in dioxane and dropwise added to the enamine at 0 °C. The reaction mixture was stirred at room temperature overnight. Then the solvent was concentrated in vacuo and the crude was filtered through silica plug (10% petroleum ether/90% ethylacetate/0.1% triethylamine) yielding 142 mg of a dark yellow solid LC–MS (M+H)<sup>+</sup>: 463.2

Bocylated compound (142 mg, 0.31 mmol) was dissolved in methanol and treated with a solution freshly prepared of MeOH/MeONa (15 mg, 0.62 mmol of Na in 1 mL of MeOH). The resulting solution was stirred at room temperature for 30 min. UPLC analysis showed the cyclization went to completion. It was diluted with H<sub>2</sub>O, neutralized with 1 M HCl and extracted with ethylacetate. The organic layer was dried over Na<sub>2</sub>SO<sub>4</sub> and concentrated in vacuo. The crude was purified by silica gel chromatography (ethylacetate/methanol gradient): final compound was obtained as a yellow solid (44 mg, 33% yield, 97% HPLC purity). <sup>1</sup>H NMR (DMSO-*d*<sub>6</sub>, 500 MHz) δ: 11.72 (bs, 1H), 7.66–7.60 (m, 2H), 7.51–7.40 (m, 3H), 5.66 (s, 1H), 5.19–5.11 (m, 2H), 4.50–4.41 (m, 2H), 3.64–3.55 (m, 2H), 1.98 (s, 9H), 1.72–1.66 (m, 2H). LC–MS (M+H)<sup>+</sup>: 431.1.

#### 4.2.2. Synthesis of 2-(2-chlorophenyl)-2,3,8,9,10,11-hexahydro-1*H*-pyrazolo[4,3':3,4]pyrido[1,2-*a*][1,4]diazepine-1,5(7*H*)-dione (**7a**)

The Boc protected compound **6a** was dissolved in DCM and 4 M HCl in dioxane was added followed by one drop of water. The reaction was stirred at room temperature for 30 min and monitored by UPLC and HPLC. When the starting material was completely consumed, the solvent was concentrated in vacuo and the residue was precipitated from methanol and diethylether. The yellow solid was filtered off and washed with small portions of diethylether. The final compound was obtained as a yellow HCl salt with 98% HPLC purity (91% yield). <sup>1</sup>H NMR (DMSO-*d*<sub>6</sub>, 500 MHz) δ: 11.07 (s, 1H), 9.57 (BS, 1H), 7.70–7.67 (m, 1H), 7.57–7.54 (m, 1H), 7.53–7.49 (m, 2H), 5.89 (s, 1H), 5.04–4.98 (m, 2H), 4.61–4.51 (m, 2H), 3.47–3.37 (m, 2H), 1.95–1.88 (m, 2H). LC–MS (M+H)<sup>+</sup>: 331.1

#### 4.3. General procedure for the synthesis of hexahydro-1,4-diazepine derivatives (*n* = 2)

##### 4.3.1. Synthesis of 10-benzyl-2-(2-chlorophenyl)-2,3,8,9,10,11-hexahydro-1*H*-pyrazolo[4,3':3,4]pyrido[1,2-*a*][1,4]diazepine-1,5(7*H*)-dione (**7c**)

Pyrazolone **1b** (643 mg, 1.88 mmol) was dissolved in CH<sub>3</sub>CN (10 mL) and amine **2** *N*-benzylpropane-1,3-diamine was added at 0 °C under N<sub>2</sub>. The reaction mixture was stirred at 0 °C for 3 h and monitored by LC–MS showing 40% of starting material left. Then DIPEA (two drops) was added and the mixture was stirred at RT for 1 h: LC–MS showed completely conversion of starting material into desired product. The solvent was concen-

trated in vacuo until dryness. The residue was dissolved in ethylacetate (10 mL), washed with saturated NaHCO<sub>3</sub> solution (5 mL \* 2), dried over Na<sub>2</sub>SO<sub>4</sub> and concentrated. The crude product was used in the following step without further manipulation (530 mg, 71% yield, 86% HPLC purity, LC–MS (M+H)<sup>+</sup>: 453.4).

The obtained enamine type **4** (530 mg, 1.2 mmol) was treated with freshly prepared MeONa in MeOH, obtained from dissolution of Na (55 mg, 2.4 mmol) in 3 mL of MeOH under N<sub>2</sub>. The solution was stirred at room temperature until disappearance of the starting enamine (1 h). The reaction mixture was concentrated in vacuum to eliminate MeOH and the crude was dissolved in ethylacetate (20 mL), extracted with water (20 mL \* 3). Then the combined inorganic layer was acidified to pH 6, extracted with ethylacetate (30 mL \* 3) and the combined organic layers were dried over Na<sub>2</sub>SO<sub>4</sub>. The crude was purified by TLC yielding a beige solid (142 mg, 28% yield, 97% HPLC purity).

The product **6** was dissolved in 2 mL MeOH and treated with 4 M HCl in MeOH (0.082 mL). Then MeOH was removed, the residue was triturated with Et<sub>2</sub>O. The combined yellow powder was dried in vacuo (103 mg, HPLC: 97%). Mp 198–200 °C. <sup>1</sup>H NMR (DMSO-*d*<sub>6</sub>, 400 MHz) δ: 10.71 (bs, 1H), 7.66–7.62 (m, 1H), 7.59–7.55 (m, 1H), 7.49–7.47 (m, 2H), 7.32–7.25 (m, 4H), 7.25–7.21 (m, 1H), 5.73 (s, 1H), 4.70–4.55 (m, 2H), 4.55–4.39 (m, 2H), 3.64 (s, 2H), 2.83 (t, *J* = 4.34 Hz, 2H), 1.69–1.61 (m, 2H). <sup>13</sup>C NMR (DMSO-*d*<sub>6</sub>, 125 MHz) δ: 161.2, 159.8, 151.6, 151.4, 144.1, 133.9, 131.7, 131.3, 130.8, 130.3, 130.0, 129.6, 129.5, 128.9, 128.2, 103.6, 91.0, 56.7, 52.4, 48.6, 47.6, 40.6, 22.4. LC–MS (M+H)<sup>+</sup>: 421.1.

Following the above procedure, and using the appropriate starting materials, compounds **7d–7o** were obtained.

##### 4.3.2. 10-Benzyl-2-(2-methoxyphenyl)-2,3,8,9,10,11-hexahydro-1*H*-pyrazolo[4,3':3,4]pyrido[1,2-*a*][1,4]diazepine-1,5(7*H*)-dione (**7d**)

Isolated as a yellow solid (94% HPLC purity). <sup>1</sup>H NMR (DMSO-*d*<sub>6</sub>, 400 MHz) δ: 7.60–7.58 (m, 2H), 7.43–7.36 (m, 5H), 7.18–7.16 (d, *J* = 8 Hz, 1H), 7.04–7.00 (t, *J* = 7.2 Hz, 1H), 5.83 (s, 1H), 5.17 (s, 2H), 4.52 (s, 2H), 4.29 (s, 2H), 3.72 (s, 3H), 3.42 (s, 2H), 2.04 (s, 2H). LC–MS (M+H)<sup>+</sup>: 417.3.

##### 4.3.3. 10-(2-Chlorobenzyl)-2-(2-chlorophenyl)-2,3,8,9,10,11-hexahydro-1*H*-pyrazolo[4,3':3,4]pyrido[1,2-*a*][1,4]diazepine-1,5(7*H*)-dione (**7e**)

Isolated as a brown solid (97% HPLC purity). <sup>1</sup>H NMR (DMSO-*d*<sub>6</sub>, 400 MHz) δ: 10.83 (bs, 1H), 7.63 (t, *J* = 2 Hz, 1H), 7.55–7.52 (m, 2H), 7.48–7.46 (m, 2H), 7.40–7.41 (m, 1H), 7.29–7.30 (m, 2H), 5.78 (s, 1H), 4.83–4.80 (m, 2H), 4.54–4.51 (m, 2H), 3.89–3.83 (m, 2H), 3.10–3.05 (m, 2H), 1.8–1.79 (m, 2H). LC–MS (M+H)<sup>+</sup>: 455.2.

##### 4.3.4. 10-(3-Chlorobenzyl)-2-(2-chlorophenyl)-2,3,8,9,10,11-hexahydro-1*H*-pyrazolo[4,3':3,4]pyrido[1,2-*a*][1,4]diazepine-1,5(7*H*)-dione (**7f**)

Isolated as a brown solid (98% HPLC purity). <sup>1</sup>H NMR (DMSO-*d*<sub>6</sub>, 400 MHz) δ: 11.01 (bs, 1H), 7.67–7.60 (m, 2H), 7.52 (t, *J* = 4.8 Hz, 2H), 7.46 (t, *J* = 4.8 Hz, 2H), 7.45–7.40 (m, 2H), 5.84 (s, 1H), 5.10–4.90 (m, 2H), 4.52–4.48 (m, 2H), 4.23–4.20 (m, 2H), 3.18–3.13 (m, 2H), 2.00–1.96 (m, 2H). LC–MS (M+H)<sup>+</sup>: 455.0.

##### 4.3.5. 10-(4-Chlorobenzyl)-2-(2-chlorophenyl)-2,3,8,9,10,11-hexahydro-1*H*-pyrazolo[4,3':3,4]pyrido[1,2-*a*][1,4]diazepine-1,5(7*H*)-dione (**7g**)

Isolated as a brown solid (98% HPLC purity). <sup>1</sup>H NMR (DMSO-*d*<sub>6</sub>, 400 MHz) δ: 7.66–7.62 (m, 3H), 7.55–7.53 (m, 1H), 7.49–7.46 (m, 4H), 5.90 (s, 1H), 5.15 (s, 2H), 5.17–5.13 (m, 2H), 4.56–4.53 (m, 2H), 4.33–4.31 (m, 2H), 4.32 (s, 2H), 3.34–3.31 (m, 2H), 2.10–2.05 (m, 2H). LC–MS (M+H)<sup>+</sup>: 455.3.

**4.3.6. 2-(2-Chlorophenyl)-10-(2-methoxybenzyl)-2,3,8,9,10,11-hexahydro-1H-pyrazolo[4',3':3,4]pyrido[1,2-a][1,4]diazepine-1,5(7H)-dione (7h)**

Isolated as a brown solid (98% HPLC purity).  $^1\text{H}$  NMR (DMSO- $d_6$ , 400 MHz)  $\delta$ : 11.17 (bs, 1H), 7.65 (d,  $J = 9.2$  Hz, 1H), 7.57–7.56 (m, 1H), 7.51–7.49 (m, 3H), 7.23 (t,  $J = 7.2$  Hz, 1H), 7.09 (d,  $J = 8.4$  Hz, 1H), 6.98 (t,  $J = 7.4$  Hz, 1H), 5.90 (s, 1H), 5.42 (bs, 1H), 5.04 (bs, 1H), 4.66 (bs, 2H), 4.29 (bs, 2H), 3.81 (s, 3H), 2.22–2.14 (m, 1H), 1.98–1.96 (m, 1H). LC–MS (M+H) $^+$ : 451.26.

**4.3.7. 2-(2-Chlorophenyl)-10-(furan-3-ylmethyl)-2,3,8,9,10,11-hexahydro-1H-pyrazolo[4',3':3,4]pyrido[1,2-a][1,4]diazepine-1,5(7H)-dione (7i)**

Isolated as a brown solid (95% HPLC purity). Mp 100–102 °C.  $^1\text{H}$  NMR (DMSO- $d_6$ , 400 MHz)  $\delta$ : 10.74 (s, 1H), 7.63 (t,  $J = 4.54$  Hz, 1H), 7.55 (t,  $J = 4.8$  Hz, 1H), 7.48–7.46 (m, 2H), 7.21 (d,  $J = 3.2$  Hz, 1H), 6.85–6.81 (m, 3H), 5.73 (s, 1H), 4.65–4.45 (m, 4H), 3.70 (s, 3H), 3.61 (s, 2H), 2.86–2.84 (m, 2H), 1.65 (s, 2H). LC–MS (M+H) $^+$ : 450.9.

**4.3.8. 2-(2-Chlorophenyl)-10-(4-methoxybenzyl)-2,3,8,9,10,11-hexahydro-1H-pyrazolo[4',3':3,4]pyrido[1,2-a][1,4]diazepine-1,5(7H)-dione (7j)**

Isolated as a brown solid (96% HPLC purity).  $^1\text{H}$  NMR (DMSO- $d_6$ , 400 MHz)  $\delta$ : 11.17 (bs, 1H), 7.75–7.63 (m, 1H), 7.59–7.59 (m, 1H), 7.60–7.58 (m, 4H), 7.06 (d,  $J = 4.4$  Hz, 2H), 5.98 (s, 1H), 5.34–5.25 (m, 2H), 5.12–5.10 (d, 2H), 4.70–4.62 (m, 2H), 4.32 (s, 2H), 3.82 (s, 3H), 3.25–3.20 (m, 2H), 2.25–2.20 (m, 1H), 2.05–2.02 (m, 1H). LC–MS (M+H) $^+$ : 451.2.

**4.3.9. 2-(2-Chlorophenyl)-10-(furan-3-ylmethyl)-2,3,8,9,10,11-hexahydro-1H-pyrazolo[4',3':3,4]pyrido[1,2-a][1,4]diazepine-1,5(7H)-dione (7k)**

Isolated as a brown solid (95% HPLC purity).  $^1\text{H}$  NMR (DMSO- $d_6$ , 400 MHz)  $\delta$ : 11.11 (bs, 1H), 7.76 (s, 1H), 7.64–7.62 (m, 1H), 7.54–7.52 (m, 1H), 7.48–7.46 (m, 2H), 6.72 (d,  $J = 2.8$  Hz, 1H), 6.50 (d,  $J = 2.8$  Hz, 1H), 5.85 (s, 1H), 4.99–4.96 (m, 2H), 4.35 (s, 2H), 3.34–3.33 (m, 4H), 2.10–1.90 (m, 2H). LC–MS (M+H) $^+$ : 411.2.

**4.3.10. 2-(2-Chlorophenyl)-10-(pyridin-3-ylmethyl)-2,3,8,9,10,11-hexahydro-1H-pyrazolo[4',3':3,4]pyrido[1,2-a][1,4]diazepine-1,5(7H)-dione (7l)**

Isolated as a yellow solid (98% HPLC purity). Mp 218–220 °C.  $^1\text{H}$  NMR (DMSO- $d_6$ , 400 MHz)  $\delta$ : 10.96 (s, 1H), 8.98 (s, 1H), 8.78 (d,  $J = 4.8$  Hz, 1H), 8.60 (d,  $J = 8$  Hz, 1H), 7.92 (t,  $J = 2$  Hz, 4H), 7.57–7.50 (m, 1H), 7.49–7.44 (m, 3H), 5.79 (s, 1H), 4.84–4.82 (m, 2H), 4.53–4.51 (m, 2H), 4.29–4.28 (m, 2H), 3.32–3.31 (m, 2H), 1.98–1.97 (m, 2H). LC–MS (M+H) $^+$ : 422.9.

**4.3.11. 2-(2-Chlorophenyl)-10-(pyridin-2-ylmethyl)-2,3,8,9,10,11-hexahydro-1H-pyrazolo[4',3':3,4]pyrido[1,2-a][1,4]diazepine-1,5(7H)-dione (7m)**

Isolated as a brown solid (98% HPLC purity). Mp 93–95 °C.  $^1\text{H}$  NMR (DMSO- $d_6$ , 400 MHz)  $\delta$ : 10.78 (s, 1H), 8.52–8.51 (m, 1H), 7.85–7.84 (m, 1H), 7.63–7.60 (m, 1H), 7.52–7.44 (m, 4H), 7.35–7.34 (m, 1H), 5.76 (s, 1H), 4.72–4.72 (m, 2H), 4.51–4.49 (m, 2H), 3.95 (s, 2H), 3.08 (s, 2H), 1.76 (s, 2H). LC–MS (M+H) $^+$ : 422.9.

**4.3.12. 2-(2-Methoxyphenyl)-10-(pyridin-2-ylmethyl)-2,3,8,9,10,11-hexahydro-1H-pyrazolo[4',3':3,4]pyrido[1,2-a][1,4]diazepine-1,5(7H)-dione (7n)**

Isolated as a brown solid (94% HPLC purity). Mp 178–180 °C.  $^1\text{H}$  NMR (DMSO- $d_6$ , 400 MHz)  $\delta$ : 8.66 (dd,  $J = 0.8, 1.6$  Hz, 1H), 8.10 (td,  $J = 1.6, 8.6$  Hz, 1H), 7.74 (d,  $J = 7.6$  Hz, 1H), 7.60 (dd,  $J = 0.8, 5.4$  Hz, 1H), 7.43 (t,  $J = 8.8, 1.2$ , 1H), 7.31 (dd,  $J = 1.2, 7.6$  Hz, 1H), 7.17 (dd,  $J = 1.2$  Hz, 8.4 Hz, 1H), 7.03 (td,  $J = 1.2, 7.6$  Hz, 1H), 5.08 (s, 1H),

4.98 (bs, 2H), 4.60–4.50 (m, 2H), 4.36 (s, 2H), 3.679 (s, 3H), 3.38 (t,  $J = 5.2, 2$  Hz), 2.00–1.90 (m, 2H). LC–MS (M+H) $^+$ : 418.6.

**4.3.13. 10-(3-Methoxybenzyl)-2-(2-methoxyphenyl)-2,3,8,9,10,11-hexahydro-1H-pyrazolo[4',3':3,4]pyrido[1,2-a][1,4]diazepine-1,5(7H)-dione (7o)**

Isolated as a yellow solid (97% HPLC purity).  $^1\text{H}$  NMR (DMSO- $d_6$ , 400 MHz)  $\delta$ : 7.46–7.38 (m, 2H), 7.35–7.33 (m, 1H), 7.307–7.282 (m, 1H), 7.18 (dd,  $J = 1.2, 8.4$  Hz, m, 2H), 7.04 (t,  $J = 7.6$  Hz, 1H), 6.97 (dd,  $J = 2, 7.6$  Hz, 1H), 5.85 (s, 1H), 5.19 (s, 2H), 4.55–4.54 (m, 2H), 4.275 (s, 2H), 3.77 (s, 3H), 3.75 (s, 3H), 3.181–3.163 (m, 2H), 2.15–1.98 (m, 2H). LC–MS (M+H) $^+$ : 447.1.

**4.4. General procedure for the synthesis of tricyclic compounds with piperazine ( $n = 1$ ) or hexahydro-1,4-diazepine ( $n = 2$ ) derivatives****4.4.1. Synthesis of 9-benzyl-2-(2-chlorophenyl)-2,3,7,8,9,10-hexahydropyrazolo[4',3':3,4]pyrido[1,2-a]pyrazine-1,5-dione (7b)**

Pyrazolone **1b** (1.88 mmol, 640 mg.) was dissolved in acetonitrile (10 mL) and cooled down to 0 °C. *N*-benzyl ethane 1,2-diamine (1.69 mmol, 254 mg) was slowly added and the reaction was stirred at 0 °C for 1 h. The solvent was concentrated in vacuo and the crude was filtered through silica plug (ethyl acetate/0.1% triethylamine) yielding a dark red oil (618 mg, 75% yield, 80% HPLC purity) which was used without further manipulation and characterization. LC–MS (M+H) $^+$ : 439.1.

The enamine deriving from the previous step (618 mg, 1.42 mmol) was dissolved in MeOH (10 mL) and treated with a freshly prepared solution of MeOH/MeONa obtained from the dissolution of Na (65 mg, 2.84 mmol, 2 equiv). The resulting solution was stirred at room temperature for 30 min: UPLC analysis showed the cyclization went to completion. It was diluted with H<sub>2</sub>O, neutralized (pH 7) with 1 M HCl. Aqueous solution was loaded onto reverse phase eluted with 100% H<sub>2</sub>O in gradient with CH<sub>3</sub>CN. The product came off with 50% of CH<sub>3</sub>CN: lyophilization of aqueous solution gave a beige solid (17 mg, 11% yield, 90% HPLC purity).  $^1\text{H}$  NMR (DMSO- $d_6$ , 500 MHz)  $\delta$ : 10.71 (s, 1H), 7.63–7.61 (m, 1H), 7.53–7.50 (m, 1H), 7.47–7.44 (m, 2H), 7.37–7.34 (m, 4H), 7.30–7.26 (m, 1H), 5.62 (s, 1H), 4.10 (s, 2H), 3.83 (t, 2H,  $J = 5.6$  Hz), 3.71 (s, 2H), 2.91 (t, 2H,  $J = 5.5$  Hz). LC–MS (M+H) $^+$ : 407.1.

**4.4.2. Synthesis of 2-(2-chlorophenyl)-2,3,7,8-tetrahydro-1H-pyrazolo[4',3':3,4]pyrido[2,1-c][1,4]oxazine-1,5(10H)-dione (11)**

Pyrazolone **1b** (1.88 mmol, 640 mg.) was dissolved in acetonitrile (10 mL) and cooled to 0 °C. Propanolamine (1.69 mmol, 103 mg) was slowly added and the reaction was stirred at 0 °C for 1 h. The solvent was concentrated in vacuo and the crude was filtered through a silica plug (ethyl acetate/0.1% triethylamine) yielding a yellow oil (521 mg, 80% yield, 86% HPLC purity) which was used without further manipulation and characterization. LC–MS (M+H) $^+$ : 386.1, 388.1.

After having washed NaH (60% mineral oil, 1.5 equiv, 53 mg) with small volumes of pentane, it was suspended in THF (1 mL) under N<sub>2</sub> and cooled down to 0 °C. Enamine **9** from the previous step (421 mg, 1.31 mmol, 1 equiv) was dissolved in THF (4 mL) and dropwise added to the mixture of NaH in THF at 0 °C under N<sub>2</sub>. The mixture was stirred for 10 min and then at RT. When the starting material had completely reacted, the reaction was diluted with water (5 mL) and neutralized with 1 M HCl. The aqueous solution was extracted several times with ethyl acetate (50 mL  $\times$  4). The combined organic phases were dried over Na<sub>2</sub>SO<sub>4</sub> and after evaporation of the solvent, the crude was dissolved in the minimum amount of ethylacetate. The precipitate was filtered off, washed with small portions of cold ethyl acetate and dried under vacuo

yielding 21 mg of a yellowish solid (91% HPLC purity, 50% yield). <sup>1</sup>H NMR (DMSO-*d*<sub>6</sub>, 500 MHz)  $\delta$ : 10.81 (s, 1H), 7.66–7.63 (m, 1H), 7.55–7.52 (m, 1H), 7.50–7.46 (m, 2H), 5.67 (s, 1H), 5.13 (s, 2H), 4.08 (t, 2H, *J* = 5.3 Hz), 3.81 (t, 2H, *J* = 5.3 Hz). LC–MS (M+H)<sup>+</sup>: 318.1.

## 4.5. Biological assays

### 4.5.1. Plasmid construction

Human Nox1 (NM\_007052.4) cDNA was cloned into the pcDNA5/TO (Invitrogen), human p22 (NM\_000101.2) was cloned into pcDNA3.1/Zeo (+) (Invitrogen) and human NOXA1 (AY255769.1) and human NOXO1 (AB097667) were cloned into the bi-cistronic pVITRO1-neo-mcs plasmid (Invivogen).

### 4.5.2. Cell culture and stable transfected cell line generation

T-REx<sup>TM</sup>-CHO cells (Invitrogen) were cultured in Ham's F12 containing 4.5 g/l glucose supplemented with 10% fetal calf serum, 2 mM glutamine, penicillin (100 U/ml), streptomycin (100  $\mu$ g/ml) and blasticidin (5  $\mu$ g/ml). Cells stably expressing functional human Nox1 (hNOX1 T-REx<sup>TM</sup>-CHO) were obtained by co-transfecting T-REx<sup>TM</sup>-CHO with human NOX1, human p22, human NOXA1 and human NOXO1 using the FuGENE 6 method (Roche, 11988387).

T-REx<sup>TM</sup>-293 cell line expressing hNox4 (hNoxOX4 T-REx<sup>TM</sup>-293) was a gift from the Department of Immunology and Pathology, University of Geneva.<sup>9</sup> hNOX4 T-REx<sup>TM</sup>-293 cells were cultured in DMEM containing 4.5 g/l glucose supplemented with 10% Fetal calf serum and penicillin (100 U/ml), streptomycin (100  $\mu$ g/ml) at 37 °C in air with 5% CO<sub>2</sub>. Human Nox1 and human Nox4 expression were induced with Tetracycline (1  $\mu$ g/ml) during 24 h prior to the membrane preparation.

### 4.5.3. Membrane preparation

Membranes from human polymorphonuclear (PMN) cells (expressing high levels of Nox2) or from cells overexpressing Nox1 or Nox4 or Nox5 were prepared as previously described.<sup>10</sup> After resuspension in sonication buffer (11% sucrose, 120 mM NaCl, 1 mM EGTA in PBS, pH 7.4 for Nox4-expressing cells) or in relax buffer (10 mM Pipes, 3 mM NaCl, 3.5 mM MgCl<sub>2</sub>, 0.1 M KCl, pH 7.4), cell were broken by sonication and centrifuged (200 g, 10 min). The supernatant was layered onto a 17/40% (w/v) discontinuous sucrose gradient and centrifuged (150,000g for 30 min). Membrane fractions were collected from the 17/40% interface and were stored at –80 °C. Protein concentration was determined with Bradford reagent.

### 4.5.4. ROS production measurement

Reactive oxygen species (ROS) production by membranes expressing human Nox1, human Nox2 or human Nox4 or by Xanthine oxidase was measured using the Amplex Red (AR) method following a slightly modified version of the manufacturer's instruction manual (Invitrogen). Briefly, membranes expressing different Nox subunits or Xanthine oxidase were incubated in PBS with Amplex Red, Horse Radish Peroxidase (HRP) and appropriate co-factors. ROS production was induced by addition of NADPH to Nox expressing membranes or by addition of Xanthine to Xanthine oxidase. Nonspecific signal was measured in the absence of membranes or in the absence of agonist. Antagonist activity of compounds was measured in the presence of increasing concentrations ranging from 1 nM to 100  $\mu$ M. After 20 min. incubation at 37 °C, ROS levels were measured using a BMG Labtech microplate reader.

### 4.5.5. Data analysis

Data were analyzed using Prism (GraphPad Software Inc., San Diego, CA). *K<sub>i</sub>* values were calculated using the Cheng-Prusoff equa-

tion and represent the average of at least three individual experiments performed in triplicate.

### 4.5.6. Oxidative metabolism

Pooled human liver microsomes (pooled male and female), pooled rat liver microsomes (male Sprague Dawley rats) were used to screen the metabolic instability resulting from phase I oxidation. Microsomes (final concentration 0.5 mg/mL), 0.1 M phosphate buffer pH 7.4, and test compound (final substrate concentration = 0.5  $\mu$ M; final DMSO concentration = 0.25%) were added to the assay plate and preincubated at 37 °C.

NADPH solution (final incubation concentration = 1 mM) was added to initiate the reaction. Each compound is incubated for 0, 5, 15, 30 and 45 min. The control (minus NADPH) was incubated for 45 min only. The reactions were stopped by the addition of 50  $\mu$ L methanol containing internal standard at the appropriate time points. The samples were centrifuged at 2500 rpm for 20 min at 4 °C to precipitate the protein. Samples were analyzed by LC/MS–MS. The percentage of compound disappearance and the in vitro intrinsic clearance was calculated according to the literature.<sup>11</sup>

### 4.5.7. Cytochrome P450 inhibition

Six human recombinant cytochrome P450 isoenzymes (BD Gentest, Woburn, MA) were tested (CYP1A2, CYP2C8, CYP2C9, CYP2C19, CYP2D6 and CYP3A4). Test compound (0.1–25  $\mu$ M) was incubated (final DMSO concentration = 0.3%) with specific species liver microsomes and NADPH in the presence of a cytochrome P450 isoform-specific probe substrate. For the CYP2C8, CYP2C9, CYP2C19, CYP2D6 and CYP3A4 specific reactions, the metabolites were monitored by mass spectrometry. CYP1A2 activity was monitored by measuring the formation of a fluorescent metabolite. A decrease in the formation of the metabolite compared to the vehicle control was used to calculate an IC<sub>50</sub> value.

### 4.5.8. Caco-2 permeability

Caco-2 cells were obtained from American type culture collection (Rockville, MD). The cells were seeded onto a Millipore Multi-screen Caco-2 plates at  $1 \cdot 10^5$  cell/cm<sup>2</sup> and grown in Dulbecco's modified Eagle's medium and media was changed every two or three days. Permeability studies were performed with the monolayers cultured for 20 days. On day 20, the monolayers were prepared by rinsing both basolateral and apical surfaces twice with HBSS at 37 °C. Prior to all experiments, the cell monolayer integrity was evaluated by *trans* epithelial electrical resistance; values greater than 800 ohm  $\cdot$  cm<sup>2</sup> were used. Hank's balanced salt solution buffer was then removed from either the apical compartment (for apical to basolateral transport; A to B) or basolateral compartment (for basolateral to apical transport; B to A) side of the monolayer and replaced with test compound dosing solutions. The permeability studies were initiated by adding an appropriate volume of solutions made by diluting 10 mM test compound in DMSO with HBSS pH 6.5 buffer to give a final test compound concentration of 10  $\mu$ M (final DMSO concentration 1%). The monolayers were then placed in an incubator at 37 °C. At the end of the incubation time (2 h), samples were taken from both the apical and basolateral compartments. Test and control compounds were quantified by LC–MS/MS cassette analysis using a 5-point calibration with appropriate dilution of the samples. The permeability coefficient (P<sub>app</sub>) was calculated according to the following equation:  $P_{app} = (dQ/dt)/(C_0 \times A)$ , where *dQ/dt* is the rate of permeation of the drug across the cell, *C*<sub>0</sub> is the donor compartment concentration at time zero and *A* is the area of the cell monolayer. *C*<sub>0</sub> is obtained from analysis of donor and receiver compartments at the end of the incubation period.

#### 4.5.9. In vivo pharmacokinetic studies in rat

These studies were conducted to estimate the plasma pharmacokinetic parameters and the oral bioavailability of compounds in the male Sprague-Dawley rat. These studies were carried out using a parallel design using six male rats. Three animals in group 1 were given 5 mg/kg iv dose; three animals in group 2 were given 10 mg/kg oral dose. Blood samples were collected from the carotid arterial cannula at various times up to 24 h following administration of compound. Plasma concentrations of compound were quantified by LC/MS/MS (LLOQ = 1.00 ng/mL). Noncompartmental methods were used for pharmacokinetic data analysis.

The vehicle used for per os administration was an aqueous solution of 0.5% CMC (carboxymethylcellulose) and 0.25% Tween 20. The vehicle used for iv injection was an aqueous solution of EDPW (10% EtOH, 10% DMA, 30% PG and 50% water).

#### 4.6. Murine curative model of bleomycin-induced lung fibrosis

##### 4.6.1. Animals

The Veterinary Office of Geneva on the Use and Care of Animals approved the animals protocols used in this study. Nine to 10-week old males C57BL/6 mice weighing 25 g were obtained from Janvier (Le Genest Saint Isle, French). Mice were housed under specific pathogen-free conditions in plastic enclosed filter-top cages (Techniplast system), five animals per cage. Animals were maintained in a 12 h light/dark cycle with ad libitum access to water and rodent laboratory chow until euthanasia.

##### 4.6.2. Study design and protocols. Instillation of Bleomycin®

For induction of Bleomycin-induced pulmonary fibrosis, Bleomycin Baxter (Pharmacie du Rondeau, Carouge, CH) was dissolved in sterile 0.9% saline on the day of IT instillation. Prior to study start animals were weighed and distributed randomly into cages. Animals were anesthetized using a solution of Ketamine/Xylazine (75 mg/kg and 8 mg/kg). A single 40 µL aliquot containing 0.0125 U of Bleomycin® diluted in normal saline was injected intratracheally using a Tridak-stepper (Millian) and a 30-gauge needle. Control mice received saline vehicle only.

##### 4.6.3. Curative treatment

Animals were randomly assigned into groups of 8 to 13 animals per group 10 days after the Bleomycin® instillation. GKT137831 and Pirfenidone were administrated at the same dose from D10 to D35 by a daily oral administration of 10 mL/kg. Compound **7c** and Pirfenidone were dissolved into a volume of 3% in DMSO followed by an aqueous solution of 0.5% CMC (carboxymethylcellulose) and 0.25% Tween 20. Pirfenidone was used as a benchmark molecule. Control groups received a daily administration of 10 mL/kg vehicle.

At the end of the experiment on D35, mice were euthanized and perfused via the right ventricle with 5 mL of saline. Lungs were carefully removed and rinsed in PBS, dried and weighed. Five lungs per group were placed in paraformaldehyde solution (PFA 4%) for histology for 24 h. Lungs were rinsed twice in PBS and processed for histology.

The remaining lungs were placed in a 1.5 mL eppendorf tubes, frozen in liquid nitrogen and stored at –80 °C until the collagen content was quantified by SIRCOL assay.

#### 4.6.4. Sircol assay for collagen quantification

Lung collagen deposition was estimated by using a dye-binding method (SIRCOL Assay, Biocolor Ltd.). Whole lung were carefully removed and homogenized in 0.5 M acid acetic. Collagen was extracted overnight at 4 °C in a mechanical shaker. After centrifugation, 100 µL of diluted supernatant was mixed with 200 µL of collagen concentrator and 1 mL of Sircol dye reagent for 30 min at room temperature in a mechanical shaker. After centrifugation, the pellet was suspended in 1 mL cuvette, with absorbance measured at 540 nm. Collagen concentrations were calculated based on the amount of Alkali reagent and vortexed to release the dye and 1 mL was transferred into a standard curve of known concentration of rat tail collagen. Data were expressed as µg of collagen per lung.

#### 4.6.5. Histology

Organs were dehydrated in successive baths containing alcohol, xylol and paraffin at 70 °C for 18 h cycle in Histokinette. They were then embedded in paraffin and cut using microtome (4 µm), then mounted on Superfrost slide. Sections were dried in a stove at 60 °C overnight and stained by hematoxylin and eosin or Masson's Trichrome for collagen staining.

#### Acknowledgments

We thank He Haiying, Cao Yafeng, Lei Jianguang (WuXi AppTec, Shanghai) and the Wuxi AppTec chemistry team for their participation to this work.

#### Supplementary data

Supplementary data associated with this article can be found, in the online version, at [doi:10.1016/j.bmc.2011.10.016](https://doi.org/10.1016/j.bmc.2011.10.016).

#### Reference and notes

- Schwartz, D. A.; Helmers, R. A.; Galvin, J. R.; Van Fossen, D. S.; Frees, K. L.; Dayton, C. S.; Burmeister, L. F.; Hunninghake, G. W. *Am. J. Respir. Crit. Care Med.* **1994**, *149*, 450.
- King, T. E., Jr.; Tooze, J. A.; Schwarz, M. I.; Brown, K. R.; Cherniack, R. M. *Am. J. Respir. Crit. Care Med.* **2001**, *164*, 1171.
- Misra, H. P.; Rabideau, C. *Mol. Cell Biochem.* **2000**, *204*, 119.
- Kim, J. A.; Neupane, J. P.; Lee, E. S.; Jeong, B. S.; Park, B. C.; Thapa, P. *Expert. Opin. Ther. Pat.* **2011** (Epub ahead of print).
- Hecker, L.; Vittal, R.; Jones, T.; Jagirdar, R.; Luckhardt, T. R.; Horowitz, J. C.; Pennathur, S.; Martinez, F. J.; Thannickal, V. J. *Nat. Med.* **2009**, *15*, 1077.
- Laleu, B.; Gaggini, F.; Orchard, M.; Fioraso-Cartier, L.; Cagnon, L.; Houngrinou-Molango, S.; Gradia, A.; Duboux, G.; Merlot, C.; Heitz, F.; Szyndralewicz, C.; Page, P. *J. Med. Chem.* **2010**, *53*, 7715.
- Page, P.; Gaggini, F.; Laleu, B. Pyrazoline dione derivatives as NADPH oxidase inhibitors WO2011/036651 A1, 2011, Genkyotex.
- Abdel-Magid, A. F.; Carson, K. G.; Harris, B. D.; Maryanoff, C. A.; Shah, R. D. *J. Org. Chem.* **1996**, *61*, 3849.
- Serrander, L.; Cartier, L.; Bedard, K.; Banfi, B.; Lardy, B.; Plastre, O.; Sienkiewicz, A.; Fórró, L.; Sclegel, W.; Krause, K. H. *Biochem. J.* **2007**, *406*, 105.
- Palicz, A.; Foubert, T. R.; Jesaitis, A. J.; Marodi, L.; McPhail, L. C. *J. Biol. Chem.* **2001**, *276*, 3090.
- Lave, T. H.; Dupin, S.; Schmitt, C.; Chou, R. C.; Jack, D.; Coassolo, P. H. *J. Pharm. Sci.* **1997**, *86*, 584.